

Structural Information on the Light-Harvesting Complex II of Green Plants That Can Be Deciphered from Polarized Absorption Characteristics

Demet Gülen,[†] Rienk van Grondelle,[‡] and Herbert van Amerongen^{*‡}

Physics Department, Middle East Technical University, Ankara, 06531, Turkey, and Department of Physics and Astronomy and Institute for Molecular Biological Sciences, Vrije Universiteit, De Boelelaan 1081, 1081 HV Amsterdam, The Netherlands

Received: October 29, 1996; In Final Form: April 29, 1997[®]

The atomic model of light-harvesting complex II of green plants (LHCII) reveals a densely packed arrangement of 12 chlorophylls and two carotenoids. At the current resolution of 3.4 Å chlorophylls can only be modeled as “naked” tetrapyrrole rings. Consequently, definitive assignments of the identities of the chlorophylls (chlorophyll *a* or chlorophyll *b*) and the directions of the transition dipole moments are obstructed. These uncertainties lead to a large number of possible configurations, and a detailed understanding of the structure–function relationship is obscured. It is demonstrated that a large reduction in the number of possible configurations and a considerable amount of additional structural information can be obtained by deciphering global features of the polarized absorption spectra within the context of exciton calculations. It is shown that only a limited number of configurations are able to explain the global features of the linear and circular dichroism spectra of LHCII. Assuming that the preliminary assignment of the identities of the 12 chlorophylls by Kühlbrandt and co-workers is correct, it is possible to deduce the most likely orientations for most of the chlorophylls. The information presented in this study on the most likely orientations will be important for a detailed understanding of the relation between the structure and spectroscopy.

Introduction

In photosynthesis about 50% of all the chlorophylls are associated with the light-harvesting complex II (LHCII). The major function of LHCII is to absorb solar photons and to transport the excitation energy to the reaction centers of mainly photosystem II, where it drives a charge separation. There is no doubt that the 3.4 Å atomic model for LHCII by Kühlbrandt, Wang, and Fujiiyoshi¹ plays an essential role in understanding the relation between structure and function. However, a detailed understanding of the functional properties is hampered, in part, by the uncertainties associated with the current model.

In the atomic model, each monomer of this C_3 symmetric complex hosts two carotenoid (Car) and 12 chlorophyll (Chl) molecules. At the current resolution, Chls can only be modeled as “naked” tetrapyrrole rings, and definitive assignments of the identities of the Chls and the directions of the transition dipole moments associated with the functionally important red and the Soret transitions are difficult.

A preliminary assignment of the identities of the Chls has been proposed based on the stoichiometry and the functional aspects of the system: seven of the 12 Chls that are closest to the two central Cars are assigned as Chl *a*, and the remaining five Chls, each of which is in close proximity to a “Chl *a*”, are assumed to be Chl *b*. This assignment provides a molecular conformation for rapid energy transfer from Chl *b* to Chl *a* and efficient quenching of Chl *a* triplets by Cars to prevent the formation of singlet oxygen. Although it is probably one of the most reasonable choices, it is still one out of 792 (=12!/7!5!) possible 7 Chl *a*–5 Chl *b* molecular conformations. Moreover, from biochemical analysis it was concluded that each monomer contains eight Chl *a* and six Chl *b* pigments,¹ so possibly two Chl's are missing.

On the other hand, the indistinguishability between the *x* and the *y* axes in the tetrapyrrole ring leaves a binary ambiguity for the dipole moment direction of each transition in the red/Soret. Therefore, for a given molecular conformation, there are 2^{12} (=4096) possible configurations for the orientational arrangement of the transition dipole moments.

With these uncertainties, any quantitative conclusions concerning the spectroscopy–structure relationship are obstructed. Important aspects of the structure–function relationship one would like to understand are the character of the excited states, the mechanism(s) of energy transfer, and the mechanisms leading to efficient quenching of the Chl triplets by Cars. Since the publication of the previous LHCII model,² in which several structural details were already apparent, there have been many spectroscopic studies, and a wealth of information on these aspects has been accumulated.^{3–12} It is an enormous challenge to correlate the structure of LHCII to its spectroscopic properties, which in turn are intimately related to the function. Considering the densely packed pigment content, relatively strong interactions among the Chls can be expected, and some of their effects have been reported by a number of spectroscopic studies.^{3–10}

A considerable amount of additional “structural” information can be obtained if the key features of the steady-state spectra are deciphered. In this respect, the sensitivity of polarized spectroscopy (linear dichroism, LD, and circular dichroism, CD) on the molecular configuration is particularly valuable. For example, the orientations of the Q_y transition dipole moments of LH2 from *R. sphaeroides* as determined by carefully analyzing its polarized absorption and fluorescence properties¹³ turned out to be in good agreement with the orientations in the recent crystal structure of LH2 from *R. acidophila*.¹⁴ Similarly, LD fingerprints are found to be very informative for suggesting a new starting point for a better understanding of the excited-state structure of the Fenna–Matthews–Olson complex of *P. aestuarii*.¹⁵

In this study (some preliminary results have already appeared in ref 16), polarized absorption spectra of the 2^{12} possible

* To whom correspondence should be addressed.

[†] Middle East Technical University.

[‡] Vrije Universiteit.

[®] Abstract published in *Advance ACS Abstracts*, August 1, 1997.

configurations of the molecular conformation suggested by Kühlbrandt are simulated within the context of exciton calculations. Those configurations are selected that yield features compatible with the most prominent polarization characteristics of the Chl *a* and the Chl *b* bands in the experimental spectra. It is shown that a large reduction in the number of configurations is feasible. The spectroscopic properties (dipole strengths and directions of transition dipole moments) of Chl *a* and Chl *b* have been determined with a relatively high degree of accuracy, but they are not known exactly and depend to some extent on the environmental conditions. Moreover, possibly two out of 14 Chls are missing in the structure. Therefore, we are not looking for a configuration that leads to calculated LD and CD spectra which agree best with the experimental spectra. Rather, we want to discard configurations that lead to calculated spectra that are in serious disagreement with the measured ones.

Methods

An exciton formalism that takes into account the interactions among all important low-lying *x*- and *y*-polarized red and Soret transitions of the Chls is numerically implemented. Excitonic stick spectra obtained on the basis of dipole–dipole interactions in the point dipole approximation are dressed with symmetric Gaussians to simulate the experiments. Several detailed representations of the exciton formalism used in the simulations may be found in the literature.¹⁷ This approach is sufficient for the current study, which only considers the global features of the polarized spectra. A more thorough approach (see e.g. ref 18) would in our opinion only be relevant at a later stage.

Simulations are carried out for a monomeric subunit of the trimeric LHCII complex since the global spectral features of “the monomer” and “the trimer” are almost identical.^{4,5} The tentative pigment assignment of Kühlbrandt et al. described above is used, and all the *y* (or *x*)-polarized transition dipole moment directions have been assigned in a binary fashion: the Q_y transition dipole moment is taken along one of the two diagonals connecting the nitrogen atoms (along NA–NC or NB–ND in the convention of the file provided by Dr. Kühlbrandt) of the tetrapyrrole rings. The uncertainties about the exact orientation of the Chls and the exact orientation of the transition dipoles with respect to the diagonals¹⁹ are neglected. The other dipole moment directions (Q_x , B_y , and B_x) are defined under the assumption that red (*Q*) and Soret (*B*) transitions with the same polarization are parallel to each other, and the *y*-polarized transitions are perpendicular to the *x*-polarized transitions.^{19,20} The Q_y transitions are designated by the unperturbed site energies, around 650 nm for Chl *b* and around 670 nm for Chl *a*, with the respective absorption strengths of approximately 16 and 23 D^2 . This choice of the dipole strengths is in agreement with the values measured in carbon tetrachloride²¹ (refractive index of 1.46). The Q_x transitions are assumed to have about 10–15% of the Q_y 's absorption strength and are placed around 635 nm (Chl *a*) and 617 nm (Chl *b*). The Soret region transitions (B_y and B_x), assumed to be degenerate and equal in absorption strength, are taken around 435 nm for the Chl *a* and 460 nm for the Chl *b*. The total Soret region absorption strengths corresponding respectively to the *a*'s and the *b*'s are changed between 50–70 and 60–80 D^2 . Reference 20 may be consulted for the choices of the Soret region parameters we give above. Gaussians of full width at half-maximum (fwhm) of 5.5–6 nm are judged reasonable at low temperatures (<77 K).^{6,8,22}

Only the globally striking characteristics of the LD spectra of the monomeric LHCII in the Q_y region are used to evaluate the simulation results (see below). In principle, one can also try to simulate the substructure in the Q_y spectral region (see

for instance the decomposition of the absorption spectrum in ref 22), but given the present uncertainties we consider such an approach to be premature.

$A_{||}$ and A_{\perp} are defined as the absorption of light with polarization parallel and perpendicular to the trimeric plane, and A is the isotropic absorption. The average reduced LD over the wavelength interval from λ_1 to λ_2 (LD_r) is then defined according to

$$LD_r = \left(\int_{\lambda_1}^{\lambda_2} [A_{\perp}(\lambda) - A_{||}(\lambda)] d\lambda \right) / \left(\int_{\lambda_1}^{\lambda_2} [A_{\perp}(\lambda) + 2A_{||}(\lambda)] d\lambda \right)$$

and its value can vary between -0.5 and 1.0 .¹³ It should be noted that the given definition of LD_r differs in two ways from the generally used definition of the reduced LD. The latter is defined per wavelength and can be obtained from the above given definition by omitting the integration. Moreover, parallel and perpendicular refer here to molecular axes instead of axes in the laboratory frame. This can be done because in ref 3 the absorption spectra with respect to the C_3 symmetry axis were determined explicitly.

The polarization characteristics of the LHCII absorption bands have been extensively analyzed in ref 3. Some important results were the following: the value of the average reduced dichroism above 660 nm (here called LD_a because this region is dominated by the Chl *a*) is around -0.3 ; between 640 and 660 nm (here called LD_b) the reduced dichroism is close to zero; on the red edge of the Chl *a* region the corresponding dipole moments on average are significantly more in plane than those on the blue side of the Chl *a* absorption region, and particularly, the dipole moments contributing to the main Chl *a* absorption band (676 nm) are oriented almost perfectly parallel to the trimeric plane. Below LD_{red} denotes the reduced LD averaged over the two redmost bands. In view of the uncertainties inherent to the directions of the transition dipole moments, comparison between the simulations and the experiments is done on the basis of relatively mild criteria. It was somewhat arbitrarily decided that only those conformations are acceptable for which $-0.50 < LD_a < -0.10$, $-0.25 < LD_b < 0.30$, and $-0.50 < LD_{red} < -0.30$. Here the margins for LD_b are chosen slightly larger because there is some contribution from Chl *a* vibronic bands in the Chl *b* Q_y region.

Results and Discussion

The reduction statistics obtained by analyzing the polarization characteristics of the absorption bands of all 2^{12} (4096) possible configurations are given in Table 1. It should be stressed that with the broad range given for the values of LD_a and LD_b we eliminate the possibilities that are certainly wrong.

The strongest reduction of possible configurations is obtained by restricting the average reduced LD in the Chl *a* region (LD_a), which leads to an approximately 10–30-fold decrease depending on the choice of the restriction criteria. Only 122 out of the 4096 possible configurations lead to a calculated value for LD_a that is smaller than -0.15 . It is striking that in all these cases the Q_y dipole moment of Chl *a7* can only adopt one orientation, whereas also Chl's *a1* and *a4* have a strong preference. Another 2–2.5-fold reduction follows if in addition the average reduced LD over the two redmost bands (LD_{red}) is restricted.

Thus, by considering only the very prominent polarization characteristics of the Chl *a* band, the reduction factor with very relaxed elimination conditions is around 20-fold, and the reduction is already as high as 80-fold with slightly more stringent, but still relatively mild, restrictions. The restriction of the average reduced LD over the Chl *b* band (LD_b) contributes only a 1.5–2-fold reduction if applied directly to all 2^{12} configurations. This factor is higher when the LD_b of the LD_a

TABLE 1: Survival Statistics for a Typical Case^a

restriction criteria ^b				no. of survivors/ reduction factor	survival statistics ^d							
LD _a	LD _{red}	LD _b	other ^c		a1	a2	a3	a4	a5	a6	a7	b3
		0.30		2871/1.43								
		0.23		2266/1.81								
	-0.30			1907/2.15								
	-0.35			1554/2.64								
-0.10				397/10.32	0.806	0.620	0.408	0.907	0.730	0.763	0.980	0.519
-0.15				122/33.57	0.902	0.672	0.328	0.992	0.844	0.820	1.0	0.566
-0.10		0.30		224/18.29	0.978	0.535	0.513	0.924	0.714	0.737	0.996	0.223
-0.15		0.23		43/95.26	1.0	0.419	0.488	1.0	0.907	0.837	1.0	0.002
-0.10	-0.30			186/22.02	0.726	0.924	0.344	0.898	0.828	0.753	0.962	0.575
-0.15	-0.30			68/60.24	0.868	0.985	0.294	0.985	0.882	0.779	1.0	0.588
-0.15	-0.35			49/83.59	0.837	0.980	0.403	0.909	0.818	0.701	0.987	0.156
-0.15	-0.30	0.23		20/204.50	1.0	1.0	0.350	1.0	0.950	0.750	1.0	0.0
-0.15	-0.35	0.25		13/315.00	1.0	1.0	0.308	1.0	1.0	0.615	1.0	0.0
-0.15	-0.30	0.30	b1	28/146.29	0.750	0.857	0.393	0.964	0.857	0.679	1.0	0.0
-0.15		0.25	b1	12/341.33	1.0	0.583	0.500	1.0	0.917	0.917	1.0	0.0

^a The following input parameters are used. The absorption strengths (in D²) are 16.5 (Q_y, Chl *b*), 23.5 (Q_y, Chl *a*), 2.8 (Q_x, Chl *a*), 1.95 (Q_x, Chl *b*), 28 (B_x = B_y, Chl *a*), 33 (B_x = B_y, Chl *b*). The respective unperturbed transition wavelengths are 650, 670, 635, 617, 435, and 460 nm. ^b See text. ^c In this column, the label *b1* indicates that the Chl *b1*'s *y*-polarized dipole moment is forced to be along NB–ND. These rows are included to demonstrate how additional experimental observations might be helpful. ^d The probability that the Chl's listed assume the *y*-polarized dipole moment directions along NA–NC. The probabilities are calculated relative to the number of survivors in each row.

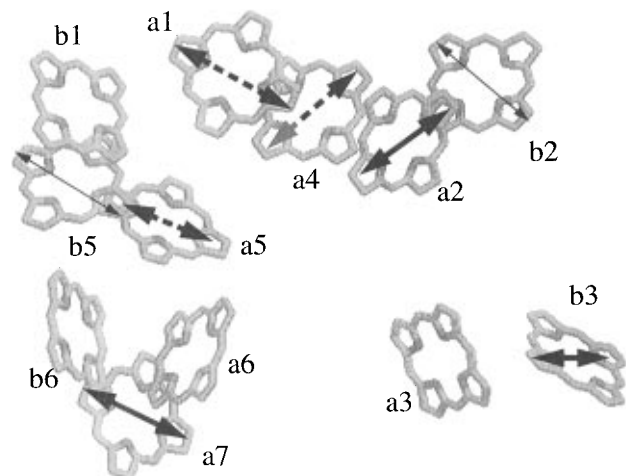


Figure 1. Calculated directions for the dipole moments of the *y*-polarized transitions of several Chl's. Shown are Chl's in a monomeric subunit of trimeric LHCII. The thick solid dipoles are determined to a very good degree of certainty even under extremely relaxed elimination criteria. The thick dashed ones are slightly less certain. No solid conclusions could be drawn about the thin solid dipoles, but a preliminary assignment is made which gives rise to a reasonable explanation of many experimental results.

+ LD_{red} survivors is restricted. In summary, the combination of the LD_a, LD_{red}, and LD_b leaves us with at most about 75 configurations, which is as low as about 15 configurations if the restrictions are somewhat tightened.

Following the elimination on the LD_a selection, the Chl *a* region configurations of the survivors are not widely scattered over the available configurational space. They are rather grouped into certain subclasses (around 10–15 out of 2⁷), in which at least four of the seven Chl *a* molecules adopt one of the two possible “*y*” directions. What is more important is that each of the restrictions used forces at least one specific Chl molecule to an almost uniquely defined orientation. This observation suggests that the average reduced LD does not strongly depend on the excitonic interactions: a point which is already discussed in ref 3. This point of view is further supported by the recent theoretical results on the Fenna–Matthews–Olson protein complex, for which some of the LD features are critically determined by the individual Bchl orientations, despite the existence of couplings that are an order of magnitude stronger than the *a*–*a* and *b*–*b* couplings of LHCII.¹⁵ This is also true for LHCII since the average reduced

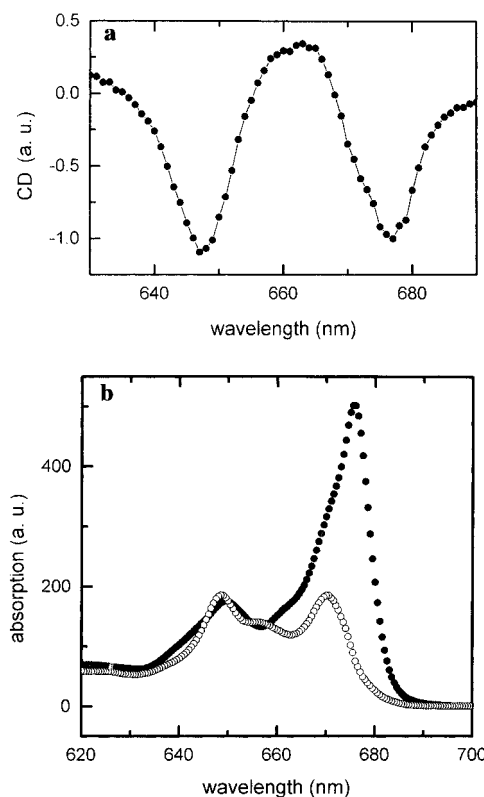


Figure 2. (a) The 77 K CD spectrum of monomeric LHCII taken from (ref 4). (b) Linearly polarized absorption spectra taken from (ref 3). They are derived from experimental absorption and linear dichroism spectra as explained in ref 3. The solid dots represent the absorption parallel to the trimeric plane (or perpendicular to the C₃ symmetry axis), and the open dots represent the absorption perpendicular to this plane (or parallel to the C₃ symmetry axis).

LD does not strongly depend on the excitonic interactions (see also ref 3). The survival statistics of Table 1 shows the Chl *a7* orientation is almost uniquely determined by the LD_a elimination, the Chl *a2* is the key molecule for determining the polarization characteristics of the redmost bands of the cases that survive the LD_a elimination, and the orientation of the Chl *b3* molecule is almost unequivocally defined by the LD_b filtering. The most undetermined Chl *a* directions are those of *a3* and *a6*. This is because the “*y*” and “*x*” axes make a similar angle with respect to the plane of the trimer. Moreover, the remaining Chl *a* molecules (1, 4, and 5) largely prefer one of

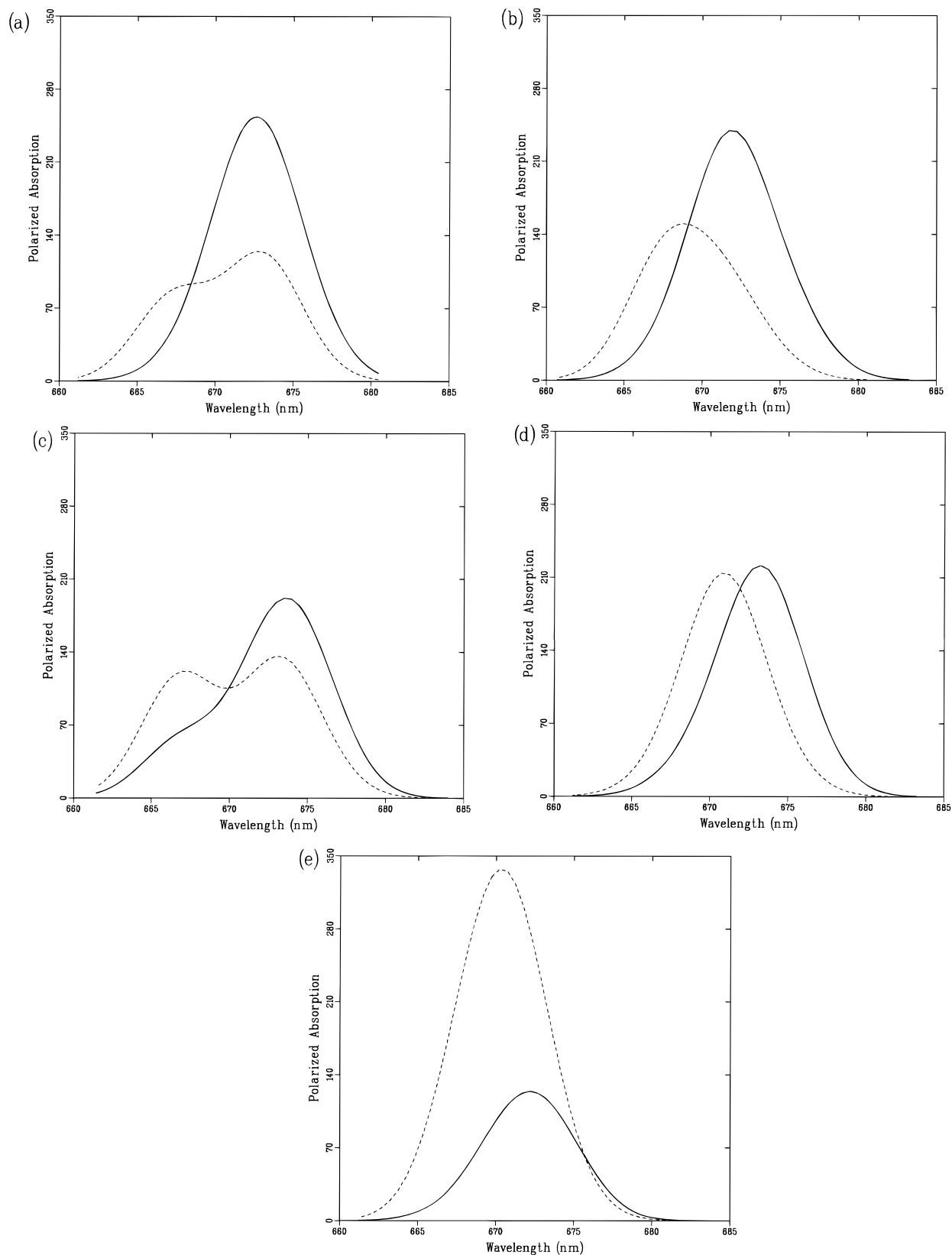


Figure 3. Simulated polarized absorption spectra of the Chl *a* absorption region for various configurations (given in arbitrary units). The solid line represents the absorption parallel to the trimeric plane (or perpendicular to the C_3 symmetry axis), and the dashed line represents the absorption perpendicular to this plane (or parallel to the C_3 symmetry axis). In all cases the transition dipole moments of all Chl *b* molecules were taken along the NB–ND diagonal. The individual Chl *a* and Chl *b* absorption strengths and the unperturbed transition energies are the same as in Table 1, and the excitonic stick transitions are dressed with symmetric Gaussians of fwhm = 5.75 nm. All simulated spectra have the same absolute scale. In panel a the *y*-polarized transition dipole moments of all the Chl *a* molecules are along the NA–NC diagonal, and in panel e all are along the NB–ND diagonal. In panel b the *y* direction for Chl *a3* is along NB–ND while for the other Chl *a* molecules they are oriented along NA–NC. Similarly, in panel c the *y* direction for Chl *a4* is along NB–ND while for the other Chl *a* molecules they are oriented along NA–NC. Similarly, in panel d only the *y* axis of Chl *a7* is along NB–ND. The value of the average reduced LD over the Chl *a* band (LD_a) is -0.154 , -0.144 , -0.061 , -0.056 , and $+0.339$ for panels a, b, c, d, and e, respectively. Throughout this figure one can clearly follow the correlation between the survival statistics (Table 1) predictions and the simulated spectral characteristics.

the two possible “y” orientations. Chls *a1* and *a4* tend to assume the preferred orientation upon LD_a filtering, and this tendency gets stronger after imposing the others. It is found that the two Chl *a* pairs, *a1*–*a4* and *a2*–*a5*, whose tetrapyrrole rings are related to each other by an approximate 2-fold symmetry tend to conserve the same symmetry also in the dipole moment orientations. Within a combinatorial restriction of LD_a, LD_{red}, and LD_b, it remains largely ambiguous whether this is also the case for the other symmetrical Chl *a* pair (*a3*–*a6*).

The most likely orientations of the y-polarized transitions based on the calculations are summarized in Figure 1. The circular dichroism (CD) of LHCII (Figure 2a) contains additional information about the polarization characteristics of the absorption bands. The CD in the Chl *a* region of the spectrum is strongly biphasic (with a crossing point around 670 nm), being positive on the short wavelength side (peaking around 665 nm) and negative on the long wavelength side (peaking around 675 nm).^{4,5} Calculated spectra could be regarded to be unacceptable if either these signs are reversed or the CD signal in the Chl *a* region is dominantly monophasic. However, we have avoided a strict elimination on the basis of CD spectra since it is known that the CD is extremely sensitive to the uncertainties in the directions of the dipole moments (as well as the inhomogeneities in the site energies).^{17,18} We have nevertheless determined how much reduction can be obtained if the key CD features are used for further elimination. It is concluded that another reduction factor of around 2 can be associated with each of the key CD features described above.

The 77 K absorption spectra A_{\parallel} and A_{\perp} as determined in ref 3 are given in Figure 2 together with the 77 K CD spectrum of monomeric LHCII.⁴ In Figure 3 we have simulated A_{\parallel} and A_{\perp} over the Chl *a* absorption band for various configurations. This figure is provided to illustrate how sensitive the spectra are to different orientations of the chlorophylls. Throughout Figure 3 one can clearly follow that the survival statistics results correlate well with the simulated spectral characteristics. (See the figure caption for more details.) Taking the y axis of all Chl *a* molecules along NA–NC gives rise to reasonable spectra whereas taking them all along NB–ND makes A_{\perp} significantly larger than A_{\parallel} , in sharp contrast to the situation in Figure 2. Starting from the situation with the y axis along NA–NC, it is seen that changing the orientation for Chl *a3* hardly changes the reduced LD whereas a reorientation of Chl *a4* and Chl *a7* leads to a significant reduction of the difference between A_{\parallel} and A_{\perp} . As far as the Chl *b* orientations are concerned, the survival statistics has only restricted the y polarization directions of Chl *b3* to the NB–ND diagonal. It is however worth mentioning that the visual inspection of the CD in the Chl *b* region indicates that for most of the reasonable cases the y-polarized transitions of Chls *b2* and *b5* in addition to *b3* are along the NB–ND diagonal (simulations not shown).

Several other features of the Chl *a* bands have been detected such as the existence of a weak redmost band with an absorption strength of approximately 1 Chl/trimer⁶ and more out-of-plane orientation of the redmost dipole(s) in comparison with the dipole moment(s) associated with the main 676 nm band. However, given the uncertainties, in both the structure and the exciton calculations, it is not realistic at this stage to impose further elimination criteria involving such details observed experimentally. Nevertheless, in order to illustrate how instrumental they could be in resolving some of the ambiguities, we have included some statistics involving comparisons between the dipole moment directions of the two redmost bands. It can be observed that this restriction assigns a preference along NB–ND to the y polarization of the otherwise undecided Chl *a6* dipole moment direction.

The structural differences between the Chl *a* and Chl *b* molecules are quite minor. Therefore, the distinction between the “y” and the “x” axes will more likely precede the Chl identification. We have also provided some statistics to illustrate how useful the incorporation of such directional information can be for narrowing down the uncertainties. (See the last two rows of Table 1.)

Concluding Remarks

As discussed, the method introduced above is successful in resolving ambiguities in specific Chl orientations, given a particular assignment of the Chl *a* and Chl *b* molecules. The question we currently consider is to what extent the uncertainties in the Chl identities can be reduced by a similar approach. The recent results from singlet–triplet transient absorption measurements¹² provide evidence for close contacts between the Chl *a* and Cars, but it cannot be excluded that some Chl *b* molecules are also located in close proximity of the central Cars. In this context, one might make use of evolutionary considerations about the complex. It has been suggested¹ that four of the central Chls related to each other by an approximate 2-fold symmetry probably form an evolutionarily conserved Chl *a* core (the ones labeled as *a1*, *a2*, *a4*, and *a5* in the current assignment). If it is furthermore assumed that three Chls that are closest to this Chl *a* core are Chl *b* (*b1*, *b2*, and *b5* in the current assignment), which would be in line with the ultrafast transfer from Chl *b* to Chl *a*,¹¹ the number of possible molecular conformations decreases drastically in the presence of stoichiometric limitations (i.e., seven Chl *a* and five Chl *b*). Also, many results from ultrafast measurements in the Q_y region will restrict the possible orientations and identities.^{11,23} We hope to address these aspects soon.

Acknowledgment. D.G. acknowledges the grants from EMBO (European Molecular Biology Organization), ESF (European Science Foundation), and NWO (The Netherlands Foundation for Scientific Research) for performing part of the work mentioned in this paper. The authors thank Dr. J. P. Dekker and Mr. E. J. G. Peterman for useful discussions. Dr. W. Kühlbrandt is acknowledged for providing the coordinates of the tetrapyrrole rings.

References and Notes

- (1) Kühlbrandt, W.; Wang, D. N.; Fujiyoshi, Y. *Nature (London)* **1994**, *367*, 614.
- (2) Kühlbrandt, W.; Wang, D. N. *Nature (London)* **1991**, *350*, 130.
- (3) Van Amerongen, H.; Kwa, S. L. S.; van Bolhuis, B. M.; van Grondelle, R. *Biophys. J.* **1994**, *67*, 837.
- (4) Nussberger, S.; Dekker, J. P.; Kühlbrandt, W.; van Bolhuis, B. M.; van Grondelle, R.; van Amerongen, H. *Biochemistry* **1994**, *33*, 14775.
- (5) Hemelrijk, P. W.; Kwa, S. L. S.; van Grondelle, R.; Dekker, J. P. *Biochim. Biophys. Acta* **1992**, *1098*, 159.
- (6) Reddy, N. R. S.; van Amerongen, H.; Kwa, S. L. S.; van Grondelle, R.; Small, G. J. *J. Phys. Chem.* **1994**, *98*, 4729.
- (7) Peterman, E. J. G.; Dekker, J. P.; van Grondelle, R.; van Amerongen, H.; Nussberger, S. *Lith. J. Phys.* **1994**, *34*, 301.
- (8) Krawczyk, S.; Krupa, Z.; Maksymiec, W. *Biochim. Biophys. Acta* **1993**, *1143*, 273.
- (9) Lokstein, H.; Leupold, D.; Voigt, B.; Nowak, F.; Ehlert, J.; Hoffman, P.; Garab, G. *Biophys. J.* **1995**, *69*, 1536.
- (10) Peterman, E. J. G.; Hobe, S.; Calkoen, F.; van Grondelle, R.; Paulsen, H.; van Amerongen, H. *Biochim. Biophys. Acta* **1996**, *1273*, 171.
- (11) Visser, H. M.; Kleima, F.; van Stokkum, I. H. M.; van Grondelle, R.; van Amerongen, H. *Chem. Phys.* **1996**, *210*, 297.
- (12) Peterman, E. J. G.; Dukker, F.; van Grondelle, R.; van Amerongen, H. *Biophys. J.* **1995**, *69*, 2670 and references therein.
- (13) Van Amerongen, H.; van Haeringen, B.; van Gorp, M.; van Grondelle, R. *Biophys. J.* **1991**, *59*, 992.
- (14) McDermott, G.; Prince, S. M.; Freer, A. A.; Hawthornwaite-Lawless, A. M.; Papiz, M. J.; Cogdell, R. J.; Isaacs, N. W. *Nature (London)* **1995**, *374*, 517.
- (15) Gülen, D. *J. Phys. Chem.* **1996**, *100*, 17683.

- (16) Gülen, D.; van Grondelle, R.; van Amerongen, H. In *Photosynthesis: From Light To Biosphere*; Proceedings of the Xth International Photosynthesis Conference, 20–25 Aug, 1995, Montpellier, France; Mathis, P., Ed.; Kluwer Academic Publishers: Dordrecht, The Netherlands, 1995; Vol. I, p 335.
- (17) Pearlstein, R. M. In *Chlorophylls*; Scheer, H., Ed.; CRC Press: Boca Raton, FL, 1991; p 1047.
- (18) Somsen, O. J. G.; van Grondelle, R.; van Amerongen, H. *Biophys. J.* **1996**, *71*, 1934.
- (19) Moog, R. S.; Kuki, A.; Fayer, M. D.; Boxer, S. G. *Biochemistry* **1984**, *23*, 1564.
- (20) Van Zandvoort, M. A. M. J.; Wrobel, D.; Lettinga, P.; van Ginkel, G.; Levine, Y. K. *Photochem. Photobiol.* **1995**, *62*, 299.
- (21) Sauer, K.; Smith, J. R. L.; Schultz, A. J. *J. Am. Chem. Soc.* **1966**, *88*, 2681.
- (22) Zucchelli, G.; Garlaschi, F. M.; Finzi, L.; Jennings, R. C. In *Photosynthesis: From Light To Biosphere*; Proceedings of the Xth International Photosynthesis Conference, 20–25 Aug, 1995, Montpellier, France; Mathis, P., Ed.; Kluwer Academic Publishers: Dordrecht, The Netherlands, 1995; Vol. I, p 179.
- (23) Özdemir, S.; Gülen, D. Manuscript in preparation.